ORIGINAL ARTICLE

Kinetics of peripheral blood neutrophils in severe coronavirus disease 2019

Mieke Metzemaekers[1†] (iD), Seppe Cambier[1†] (iD), Marfa Blanter[1], Jennifer Vandooren[2] (iD),
Ana Carolina de Carvalho[1,3,4] (iD), Bert Malengier-Devlies[2], Lore Vanderbeke[5], Cato Jacobs[6],
Sofie Coenen[7], Erik Martens[2], Noëmie Pörtner[1], Lotte Vanbrabant[1], Pierre Van Mol[8],
Yannick Van Herck[9], Nathalie Van Aerde[10], Greet Hermans[10], Jan Gunst[10], Alexandre Borin[3],
Bruna Toledo N Pereira[4], Arilson Bernardo dos SP Gomes[4] (iD), Stéfanie Primon Muraro[11],
Gabriela Fabiano de Souza[11], Alessandro S Farias[12], José Luiz Proenca-Modena[11,12],
Marco Aurélio R Vinolo[4,12], the CONTAGIOUS Consortium, Pedro Elias Marques[1] (iD),
Carine Wouters[2,13,14] (iD), Els Wauters[15] (iD), Sofie Struyf[1] (iD), Patrick Matthys[2] (iD),
Ghislain Opdenakker[2] (iD), Rafael Elias Marques[3] (iD), Joost Wauters[6] (iD), Mieke Gouwy[1†] (iD) & Paul Proost[1†] (iD)

[1]Laboratory of Molecular Immunology, Department of Microbiology, Immunology and Transplantation, Rega Institute, KU Leuven, Leuven, Belgium
[2]Laboratory of Immunobiology, Department of Microbiology, Immunology and Transplantation, Rega Institute, KU Leuven, Leuven, Belgium
[3]Brazilian Center for Research in Energy and Materials - CNPEM, Brazilian Biosciences National Laboratory, Campinas, LNBio, Brazil
[4]Laboratory of Immunoinflammation, Department of Genetics, Microbiology and Immunology, Institute of Biology, University of Campinas (UNICAMP), Campinas, Brazil
[5]Laboratory of Clinical Bacteriology and Mycology, Department of Microbiology, Immunology and Transplantation, KU Leuven, Leuven, Belgium
[6]Laboratory for Clinical Infectious and Inflammatory Disorders, Department of Microbiology, Immunology and Transplantation, KU Leuven, Leuven, Belgium
[7]Division of Pediatrics, University Hospitals Leuven, Leuven, Belgium
[8]Laboratory of Translational Genetics, Department of Human Genetics, VIB-KU Leuven, Leuven, Belgium
[9]Laboratory of Experimental Oncology, Department of Oncology, KU Leuven, Leuven, Belgium
[10]Laboratory of Intensive Care Medicine, Department of Cellular and Molecular Medicine, KU Leuven, Leuven, Belgium
[11]Laboratory Emerging Viruses, Department of Genetics, Microbiology and Immunology, Institute of Biology, University of Campinas (UNICAMP), Campinas, Brazil
[12]Experimental Medicine Research Cluster (EMRC), University of Campinas (UNICAMP), Campinas, Brazil
[13]Division of Pediatric Rheumatology, University Hospitals Leuven, Leuven, Belgium
[14]European Reference Network for Rare Immunodeficiency, Autoinflammatory and Autoimmune Diseases (RITA) at University Hospitals Leuven, Leuven, Belgium
[15]Laboratory of Respiratory Diseases and Thoracic Surgery (BREATHE), Department of Chronic Diseases and Metabolism, KU Leuven, Leuven, Belgium

Correspondence

P Proost, Laboratory of Molecular
Immunology, Rega Institute,
KU Leuven, Herestraat 49 Box 1042,
B-3000 Leuven, Belgium.
E-mail: paul.proost@kuleuven.be

†Equal contribution as first or senior
author.
Additional Contagious consortium
members are shown in Appendix 1.

Abstract

Objectives. Emerging evidence of dysregulation of the myeloid cell compartment urges investigations on neutrophil characteristics in coronavirus disease 2019 (COVID-19). We isolated neutrophils from the blood of COVID-19 patients receiving general ward care and from patients hospitalised at intensive care units (ICUs) to explore the kinetics of circulating neutrophils and factors important for neutrophil migration and activation. **Methods.** Multicolour flow cytometry was exploited for the analysis of neutrophil differentiation and activation markers. Multiplex and ELISA technologies were used for the quantification of protease, protease inhibitor, chemokine and cytokine concentrations in

plasma. Neutrophil polarisation responses were evaluated microscopically. Gelatinolytic and metalloproteinase activity in plasma was determined using a fluorogenic substrate. Co-culturing healthy donor neutrophils with severe acute respiratory syndrome coronavirus 2 (SARS-CoV-2) allowed us to investigate viral replication in neutrophils. **Results.** Upon ICU admission, patients displayed high plasma concentrations of granulocyte–colony-stimulating factor (G-CSF) and the chemokine CXCL8, accompanied by emergency myelopoiesis as illustrated by high levels of circulating CD10⁻, immature neutrophils with reduced CXCR2 and C5aR expression. Neutrophil elastase and non-metalloproteinase-derived gelatinolytic activity were increased in plasma from ICU patients. Significantly higher levels of circulating tissue inhibitor of metalloproteinase 1 (TIMP-1) in patients at ICU admission yielded decreased total MMP proteolytic activity in blood. COVID-19 neutrophils were hyper-responsive to CXCL8 and CXCL12 in shape change assays. Finally, SARS-CoV-2 failed to replicate inside human neutrophils. **Conclusion.** Our study provides detailed insights into the kinetics of neutrophil phenotype and function in severe COVID-19 patients, and supports the concept of an increased neutrophil activation state in the circulation.

Keywords: neutrophil, COVID-19, chemokine, cytokine, protease, emergency myelopoiesis

INTRODUCTION

The pandemic of COVID-19 and SARS-CoV-2, first identified in Wuhan (China) in December 2019, has resulted in over 115 million cases and more than 2.5 million deaths (WHO, covid19.who.int, as of March 2021). SARS-CoV-2 is a novel coronavirus of zoonotic origin that uses angiotensin-converting enzyme II (ACE2) as main receptor.[1] The majority of patients remain either asymptomatic or develop mild clinical symptoms such as fever, shortness of breath, cough, myalgia and fatigue.[2–4] However, 10–20% of the patients develop severe viral pneumonia and acute respiratory distress syndrome (ARDS), associated with respiratory failure.[2,3] Often, admission to intensive care units (ICUs) and mechanical ventilation are needed, and a considerable proportion of patients evolve to multiple-organ failure and eventually succumb.[5] Patients suffering from severe COVID-19 frequently have increased coagulopathy and may develop thrombotic events and neurological symptoms.[6,7] Common comorbidities such as hypertension, diabetes and asthma, as well as older age, are considered risk factors for severe and potentially fatal COVID-19.[4,8]

Severe COVID-19 cases present with a systemic inflammatory response accompanied by elevated levels of acute-phase reactants, cytokines and chemokines [e.g. C-reactive protein (CRP), soluble IL-2 receptor (IL-2R), IL-6, CXCL8, CCL2, CCL5, IL-10 and tumor necrosis factor (TNF)-α], the latter being referred to as cytokine storm.[4,9–11] White blood cell analysis revealed that a dysregulated host immune response features severe COVID-19. Abnormally low lymphocyte (especially T-lymphocytes) counts, as well as lower percentages of monocytes, basophils and eosinophils, have been described in (severe) COVID-19 cases.[4,7,9,10,12] Moreover, severe cases have higher neutrophil counts and a higher neutrophil-to-lymphocyte ratio (NLR),[4,5] which appeared as an independent biomarker predicting critical illness and poor prognosis.[13–15]

Neutrophils are highly versatile granulocytes constituting 50–70% of all peripheral blood leucocytes in humans and are the first responders to infection and tissue damage.[16] After recruitment to sites of infection and inflammation by the local action of chemokines (e.g. CXCL8), neutrophils can phagocytose and kill pathogens, release cytotoxic compounds and degradative enzymes, produce reactive oxygen species (ROS)

and expel neutrophil extracellular traps (NETs)[17–19] Moreover, phenotypically distinct neutrophil subpopulations or divergently polarised cells with functional diversity were recently identified under homeostatic and pathological conditions.[20,21] Inappropriate neutrophil activation (hyperactivation) can lead to excessive inflammation and collateral injury to (healthy) tissue as seen in subjects with several (lung) inflammatory diseases.[21,22]

Given the fact that circulating neutrophils are increased both in absolute numbers and in percentage in patients with severe COVID-19, we collected blood samples from COVID-19 patients hospitalised in dedicated general wards or in ICUs, and characterised neutrophils at phenotypical and functional levels during disease evolution. We compared the parameters with those from healthy volunteers.

RESULTS

Elevated levels of neutrophil-mobilising and neutrophil-activating factors in plasma from patients with COVID-19

Cytokine/chemokine levels were quantified in plasma from healthy controls and COVID-19 patients during the disease course. Plasma G-CSF levels were significantly higher in patients hospitalised in general wards and at ICU days 1 and 7 as compared to levels detected in healthy donors (Figure 1a). Upon discharge from the ICU, G-CSF plasma concentrations from most ICU patients were decreased to levels resembling those detected in healthy controls. Circulating granulocyte–macrophage colony-stimulating factor (GM-CSF) concentrations were < 1 pg mL^{-1} for most donors, and no differences between the study groups were detected (data not shown). The levels of CXCL12α, known to retain immature neutrophils in the bone marrow microenvironment,[23] peaked in the bloodstream after 1 week at ICU (Figure 1b). A tendency for increased CXCL12α was observed for other patient groups (Figure 1b). In contrast to the unaltered levels of the neutrophil chemoattractants CXCL1 and CXCL5, the most powerful human neutrophil-attracting chemokine CXCL8 was significantly more abundant in plasma from ICU and ward patients as compared to healthy donors (Figure 1c–e). Similar to G-CSF concentrations, CXCL8 levels significantly decreased towards ICU

discharge. Compared to healthy controls, COVID-19 patients showed significantly higher plasma levels of the highly potent CXCR3 ligands CXCL10 and CXCL11 (Figure 1f, g). Moreover, the activity in plasma of CD26/dipeptidyl peptidase IV (DPP4), a highly specific serine protease that inactivates CXCL10, CXCL11 and CXCL12 within minutes,[24] was lower in all patient groups than in healthy controls (Figure 1h). Altogether, these results show the excessive release of neutrophil-activating and neutrophil-mobilising factors during severe COVID-19, setting the stage for a scenario of neutrophil hyperactivation.

In order to evaluate the responsiveness of neutrophils from COVID-19 patients, a microscopic evaluation of blood neutrophil polarisation was performed in the presence or absence of pro-inflammatory mediators. As expected, few neutrophils from COVID-19 patients and healthy controls were polarised directly after isolation (baseline) or upon exposure to vehicle (Figure 2a, b). Remarkably, at ICU day 7 (but not at ICU admission), neutrophils were hyper-responsive to CXCL8 and CXCL12α in comparison with control cells (Figure 2c–e). No significant polarisation was elicited with TNF-α or CXCL10 (Figure 2f–h). No significant differences in polarisation responses were seen if neutrophils from healthy donors were exposed to plasma from COVID-19 patients *versus* plasma from healthy subjects (Figure 2i).

Altered levels of circulating proteases indicate neutrophil hyperactivation in patients with severe COVID-19

Neutrophils are packed with readily mobilisable granules containing pre-made inflammatory mediators. Among these pre-synthesised effector molecules are the serine protease neutrophil elastase and neutrophil gelatinase or matrix metalloproteinase-9 (MMP-9). We monitored the plasma levels of these enzymes to gain insight into the activation state of circulating neutrophils (Table 1). Neutrophil elastase concentrations were significantly enhanced in plasma from ICU patients as compared to healthy volunteers, indicating peripheral neutrophil activation in these patients (Figure 3a). The highest neutrophil elastase levels were detected upon ICU admission (Figure 3a). These observations are in line with the previously reported enhanced myeloperoxidase (MPO) levels in COVID-19 plasma.[25] A trend towards enhanced neutrophil
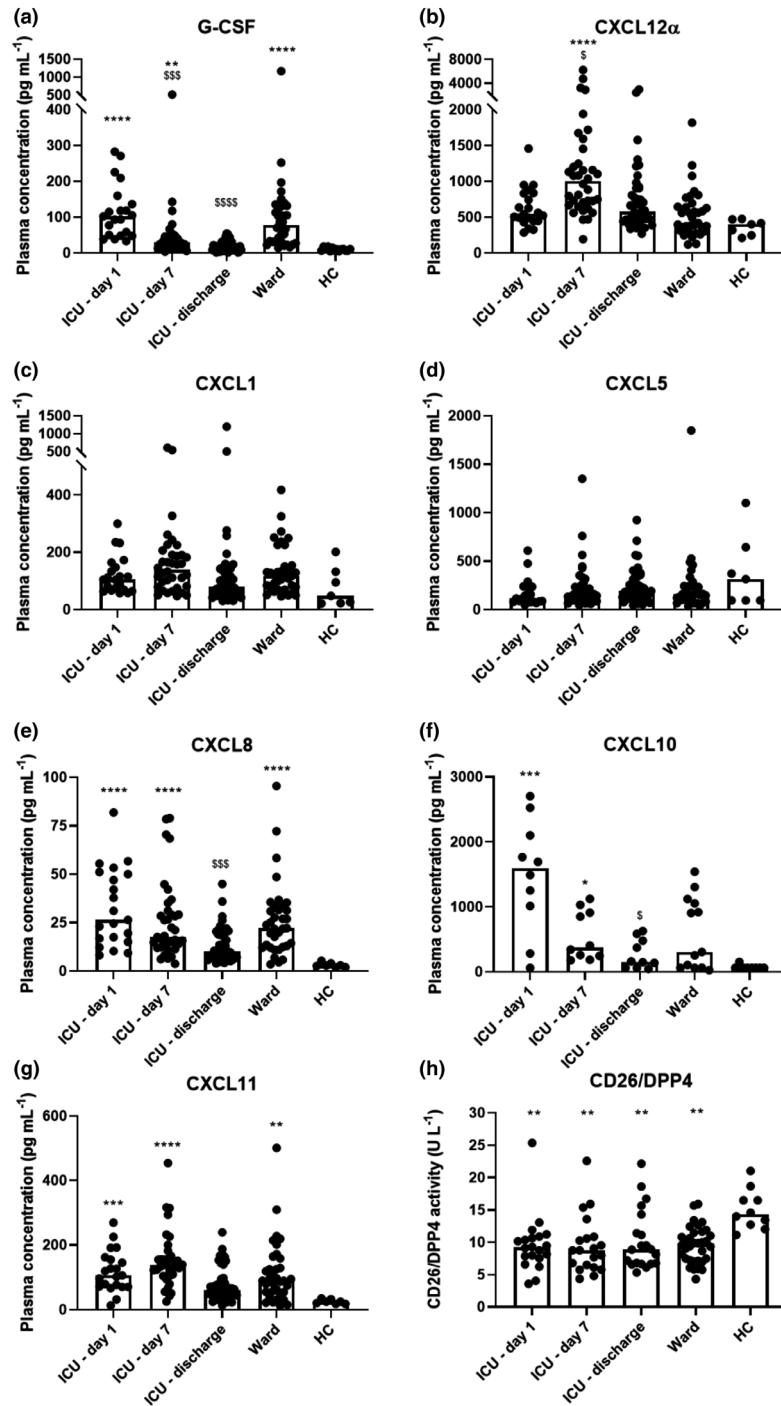
Figure 1. Quantification of neutrophil-mobilising and neutrophil-activating factors in plasma from patients with COVID-19. Multiplex technology was used to measure concentrations of **(a)** G-CSF, **(b)** CXCL12α, **(c)** CXCL1, **(d)** CXCL5, **(e)** CXCL8, **(f)** CXCL10 and **(g)** CXCL11 in plasma samples from COVID-19 patients who stayed at the ICU [samples were collected during the first 48 h after admission (ICU – day 1; $n \geq 10$), after one week (ICU – day 7; $n \geq 10$) and upon discharge from the ICU (ICU – discharge; $n \geq 10$)], COVID-19 patients who were hospitalised in general wards (ward; $n \geq 13$) and healthy controls (HC; $n \geq 7$). Moreover, **(h)** CD26/DPP4 enzyme activity was determined in a substrate conversion assay. Bars indicate the median plasma cytokine/chemokine concentration **(a–g)** or CD26 activity **(h)** for each study group. Results were statistically analysed by the Kruskal–Wallis with Dunn's multiple comparisons tests. *$P \leq 0.05$; **$P \leq 0.01$; ***$P \leq 0.001$; ****$P \leq 0.0001$ for statistical differences between patients and controls. $P \leq 0.05$; $$$P \leq 0.001$; $$$$P \leq 0.0001$ for statistical differences between ICU – day 1 and other patient groups.

Figure 2. Polarisation responses of peripheral blood neutrophils from patients with COVID-19. Neutrophils and plasma were collected from the peripheral blood of COVID-19 patients who stayed at the ICU [samples were collected during the first 48 h after admission (ICU – day 1; $n \geq 7$), after one week (ICU – day 7; $n \geq 5$) and upon discharge from the ICU (ICU – discharge; $n \geq 7$)], COVID-19 patients who were hospitalised in general wards (ward; $n = 9$) and healthy controls (HC; $n = 6$). Neutrophils were resuspended in HBSS buffer, incubated in the presence of a chemotactic stimulus and fixed, upon which the percentage of polarised cells (as determined by the cellular shape) was determined microscopically. **(a)** Baseline polarisation was determined by fixing the cells immediately after purification. Stimulus-induced polarisation was determined by incubating the cells for 3 min in the presence of the following stimuli: **(b)** vehicle; **(c)** CXCL8 (5 ng mL^{-1}); **(d)** CXCL8 (12.5 ng mL^{-1}); **(e)** CXCL12 (300 ng mL^{-1}); **(f)** TNF-α (50 ng mL^{-1}); **(g)** CXCL10 (100 ng mL^{-1}); and **(h)** CXCL10 (300 ng mL^{-1}). Moreover, **(i)** healthy donor neutrophils were treated with plasma from COVID-19 patients or healthy donors. Results are represented as percentage of polarised cells and were statistically analysed by the Kruskal–Wallis with Dunn's multiple comparisons tests. *$P \leq 0.05$ for statistical differences between groups indicated by horizontal lines.

Table 1. Overview of cytokines, chemokines, enzymes, enzyme inhibitors and enzymatic activities in plasma from COVID-19 patients

	ICU – day 1	ICU – day 7	ICU – discharge	Ward	HC
G-CSF (pg mL^{-1})	102.0 (49.1–147.9)****	28.6 (14.9–44.6)**,$$$	16.4 (8.3–26.9)$$$	78.3 (31.7–130.0)****	10.1 (6.6–14.4)
CXCL1 (pg mL^{-1})	104.2 (68.2–155.7)	139.0 (79.3–191.1)	79.1 (53.8–140.7)	117.4 (72.6–153.8)	47.8 (22.4–132.2)
CXCL5 (pg mL^{-1})	114.8 (82.7–237.7)	156.4 (115.7–271.2)	191.8 (120.0–333.6)	160.5 (101.6–246.3)	313.8 (94.3–644.0)
CXCL8 (pg mL^{-1})	26.4 (15.9–50.6)****	17.8 (12.7–30.6)****	10.2 (7.4–20.0)***	22.1 (12.4–33.6)****	2.8 (2.0–4.0)
CXCL10 (pg mL^{-1})	1593.0 (830.5–2207.0)***	374.5 (231.8–941.5)*	154.0 (61.0–507.8)$	307.0 (62.0–1088.0)	61.0 (61.0–61.0)
CXCL11 (pg mL^{-1})	106.4 (71.5–158.7)***	139.2 (104.5–163.7)****	60.9 (41.5–91.7)	90.0 (54.1–158.9)**	24.5 (18.3–32.8)
CXCL12α (pg mL^{-1})	542.1 (446.1–834.9)	1000.0 (677.7–1402.0)****,$	577.5 (453.8–880.1)	417.0 (311.1–646.3)	400.3 (246.6–469.2)
NE (ng mL^{-1})	83.7 (39.7–114.0)***	58.4 (33.6–139.3)***	40.3 (26.2–116.8)*	35.9 (25.6–63.9)	18.5 (15.1–23.4)
TIMP-1 (ng mL^{-1})	195.1 (118.0–242.3)***	159.7 (62.5–227.1)	116.2 (62.5–231.5)	90.7 (62.5–215.3)	62.5 (62.5–73.2)
TIMP-1/MMP-9 complexes (ng mL^{-1})	12.5 (3.5–42.7)	13.1 (3.5–47.1)*	6.6 (3.5–57.3)*	3.5 (3.5–3.5)	3.5 (3.5–3.5)
α2M (μg mL^{-1})	2214 (1333–4708)	2603 (761–5444)	2205 (1181–3729)	4391 (2143–8953)	1598 (1057–2217)
CD26/DPP4 activity (U L^{-1})	9.2 (7.6–10.8)**	8.8 (6.2–10.8)**	8.9 (6.7–13.6)**	9.7 (7.2–11.5)**	14.3 (12.6–17.0)
Total gelatinolytic activity (fluorescence units)	15 407 (11 243–16 754)	15 040 (11 247–18 914)	14 019 (11 220–17 980)	13 905 (11 739–16 245)	11 716 (10 023–12 846)
Non-metalloproteinase-derived gelatinolytic activity (fluorescence units)	9549 (8161–14 255)	13 702 (11 833–16 941)****	11 383 (10 038–13 871)	10 363 (7911–12 813)	9744 (8221–11 470)
Total MMP proteolytic activity (fluorescence units)	26 326 (20 307–33 665)***	46 658 (29 374–61 781)	49 674 (36 294–57 729)	30 692 (23 714–43 043)**	59 663 (48 039–70 488)
MMP activity with metalloproteinase inhibitor EDTA (fluorescence units)	14 536 (13 429–18 318)	19 541 (15 313–30 808)	16 302 (13 802–21 429)	18 385 (15 436–24 946)	15 172 (12 496–18 120)

Data are displayed as median (IQR). Results were statistically analysed by the Kruskal–Wallis with Dunn's multiple comparisons tests. α2M, alpha-2-macroglobulin; DPP4, dipeptidyl peptidase 4; G-CSF, granulocyte colony-stimulating factor; MMP, matrix metalloproteinase; NE, neutrophil elastase; TIMP-1, tissue inhibitor of metalloproteinase 1.

*$P \leq 0.05$.

**$P \leq 0.01$.

***$P \leq 0.001$.

****$P \leq 0.0001$ for statistical differences between patients and controls.

$$P \leq 0.05$.

$$$P \leq 0.001$.

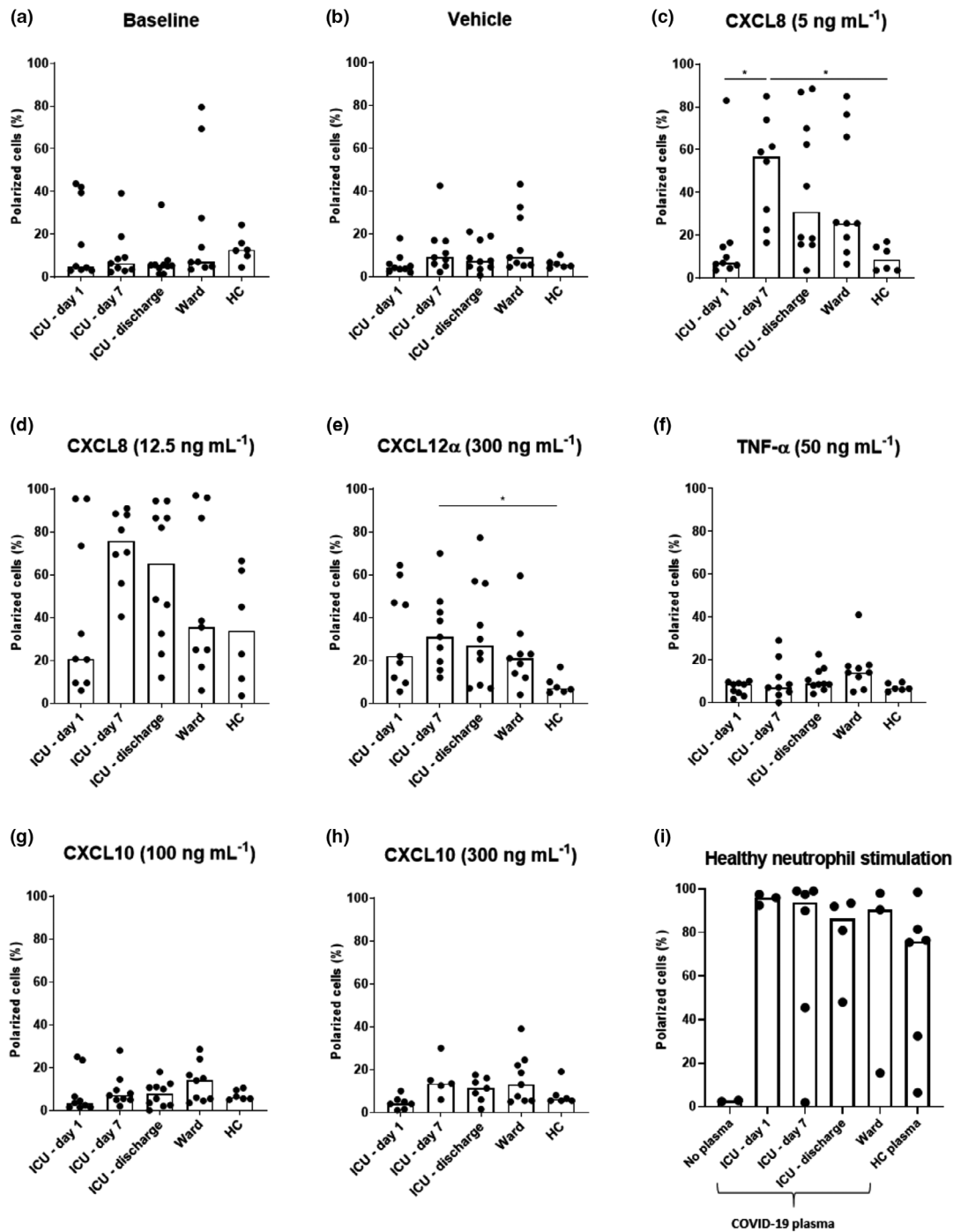$$$$$P \leq 0.0001$ for statistical differences between ICU – day 1 and other patient groups.
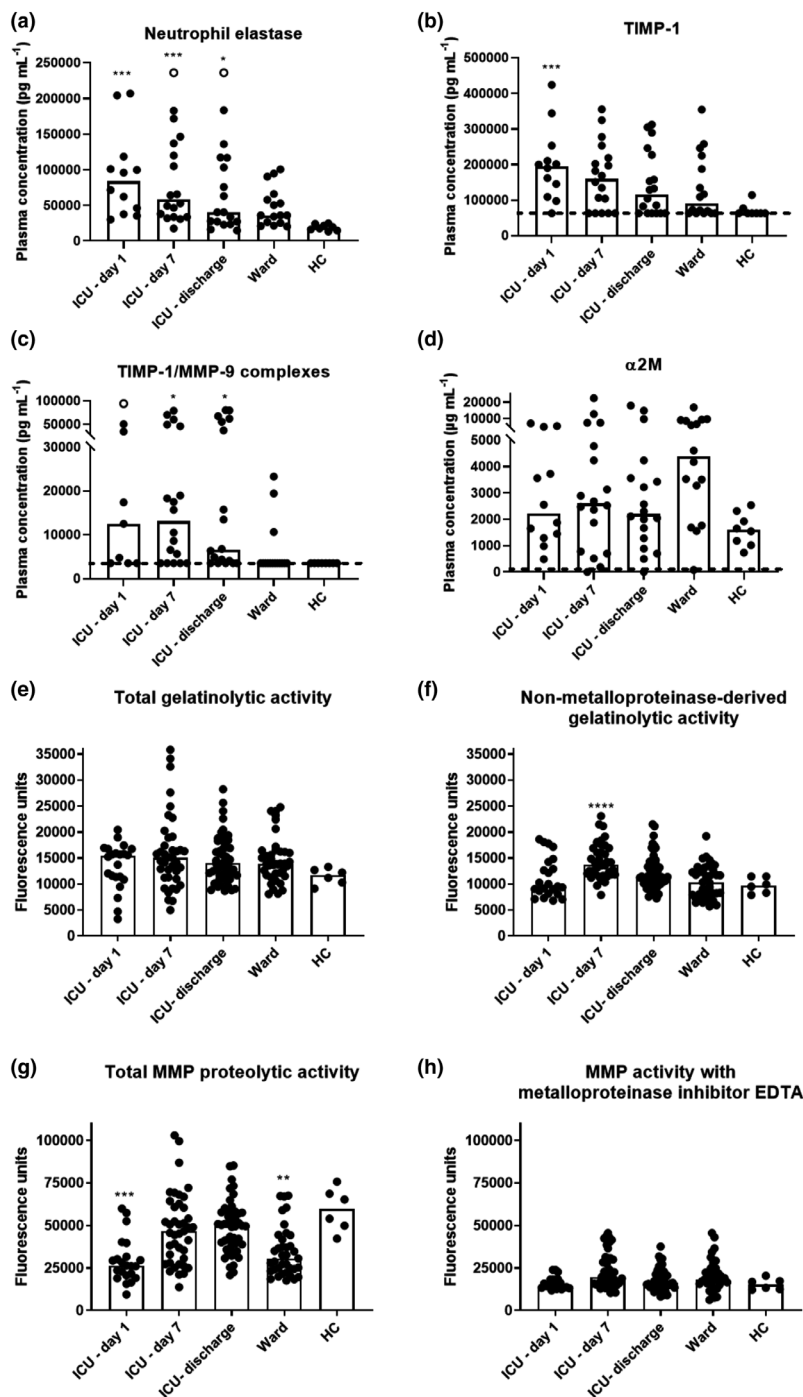
Figure 3. Quantification of proteases, protease inhibitors and enzymatic activity in plasma from patients with COVID-19. Plasma samples were collected from patients who stayed at the ICU [samples were collected during the first 48 h after admission (ICU – day 1; $n \geq 9$), after one week (ICU – day 7; $n \geq 18$) and upon discharge from ICU (ICU – discharge; $n \geq 18$)], COVID-19 patients who were hospitalised in general wards (ward; $n \geq 16$) and healthy controls (HC; $n \geq 6$). ELISA technology was used to determine concentrations of **(a)** neutrophil elastase, **(b)** TIMP-1, **(c)** TIMP-1/MMP-9 complexes and **(d)** α-2-macroglobulin (α2M). In addition, **(e)** total gelatinolytic activity present in patient plasma, as determined by the degradation of a fluorogenic gelatine substrate, **(f)** gelatinolytic activity in patient plasma in the presence of the metalloproteinase inhibitor EDTA, **(g)** total MMP activity in patient plasma, as determined by the degradation of a fluorogenic MMP substrate, and **(h)** MMP activity in patient plasma in the presence of the metalloproteinase inhibitor EDTA were measured. Bars indicate the median value for each study group. The dashed lines indicate the lower detection limits. Open symbols indicate values above the upper detection limit. Results were statistically analysed by the Kruskal–Wallis with Dunn's multiple comparisons tests. $*P \leq 0.05$; $**P \leq 0.01$; $***P \leq 0.001$; $****P \leq 0.0001$ for statistical differences between patients and controls.

elastase levels was found in plasma from ward patients (Figure 3a). Interestingly, as compared to healthy controls, the level of circulating TIMP-1 (an endogenous metalloproteinase inhibitor) was significantly higher in ICU patients at the time of admission, and a tendency towards elevated TIMP-1 concentrations was detected in all other patient groups (Figure 3b). TIMP-1/MMP-9 complexes were significantly more abundant in plasma from ICU patients (Figure 3c). Plasma concentrations of the pan proteinase inhibitor alpha-2-macroglobulin (α2M) were found highly variable within the different study groups. Although no significant differences were detected between groups, some patients presented with three- to 10-fold higher α2M concentrations than healthy controls (Figure 3d).

Given that neutrophil elastase and MMP-9 are proteases with gelatinolytic activity, we measured the gelatinolytic activity in patient plasma (Table 1). Although no significant differences were found in total gelatinolytic activity, non-metalloproteinase-derived gelatinolytic activity was significantly increased in plasma from COVID-19 patients seven days after admission (Figure 3e, f). Interestingly, total MMP activity was significantly decreased in plasma from COVID-19 patients upon admission to ICU and general wards (Figure 3g, h). In conclusion, the products of activated neutrophils and non-metalloproteinase-derived gelatinolytic activity are increased in the blood from patients with severe COVID-19, whereas increased TIMP-1 levels may contribute to counterbalancing the increases in MMP-9.

Evidence for immature, activated neutrophils in peripheral blood from patients with severe COVID-19

Peripheral blood neutrophils were examined for the expression of adhesion molecules, activation/maturation markers and chemoattractant receptors using multicolour flow cytometry. Phenotypical characterisation of neutrophils revealed the presence of immature, activated cells in peripheral blood from COVID-19 patients (Figure 4). Upon ICU admission, 45-90% of blood neutrophils were immature as evidenced by the lack of CD10 expression and the reduced levels of the low-affinity FcγR CD16[26,27] (Figure 4a, b). These observations indicate a situation of emergency myelopoiesis.[16,28] In the course of their ICU stay, COVID-19 patients gradually acquired a higher percentage of mature neutrophils in the circulation, as the CD10$^+$ population increased (Figure 4a). However, for the vast majority of patients, the relative abundance of mature neutrophils was still lower than that of healthy controls (Figure 4a). Plasma levels of G-CSF correlated inversely with the percentage of mature neutrophils (Supplementary figure 1).

During the ICU stay, multiple signs of neutrophil activation were observed. The chemokine receptor CXCR2, but not CXCR1, was significantly less abundant on patient neutrophils at ICU day 1 and day 7 as compared to controls (Figure 4c, d). As expected, most patients did not present any alterations in the expression levels of the chemokine receptors CXCR3 and CXCR4 during infection (Supplementary figure 2a and b). Expression of complement receptor C5aR was significantly lower upon ICU admission as compared to healthy donors (Figure 4e). Moreover, increased CD66b levels were detected at the beginning of the ICU stay versus discharge (Figure 4f). Complement receptor 1 (CR1) or CD35 was significantly more abundant on neutrophils from ICU patients at day 7 of hospitalisation as compared to admission (Figure 4g). The expression of the tetraspanin CD63, a surface receptor for TIMP-1,[29] was increased after one week of hospitalisation at ICU as compared to discharge (Figure 4h). No expression of CD49d, IL-1R1, CCR1, CCR2 or ICAM-1 was detected in any group. For IL-1R2, BLTR1, CD11b, CD11c, CD15, CD62L, FPR1 and HLA-DR, no significant differences were found between patients and controls, although a tendency towards increased numbers of HLA-DR positive cells was seen in the circulation from COVID-19 patients (Supplementary figure 2c–j).

SARS-CoV-2 fails to replicate in human neutrophils in vitro

A pertinent question in the case of COVID-19 is whether neutrophils may propagate the virus. Indeed, in view of the phenotypical and functional alterations of peripheral blood neutrophils from COVID-19 patients, it was imperative to investigate possible disease-promoting effects. To explore whether SARS-CoV-2 is capable of infecting neutrophils, we incubated freshly isolated neutrophils from healthy donors with SARS-CoV-2 or vehicle in vitro. SARS-CoV-2 infectivity and ability to replicate in cells were
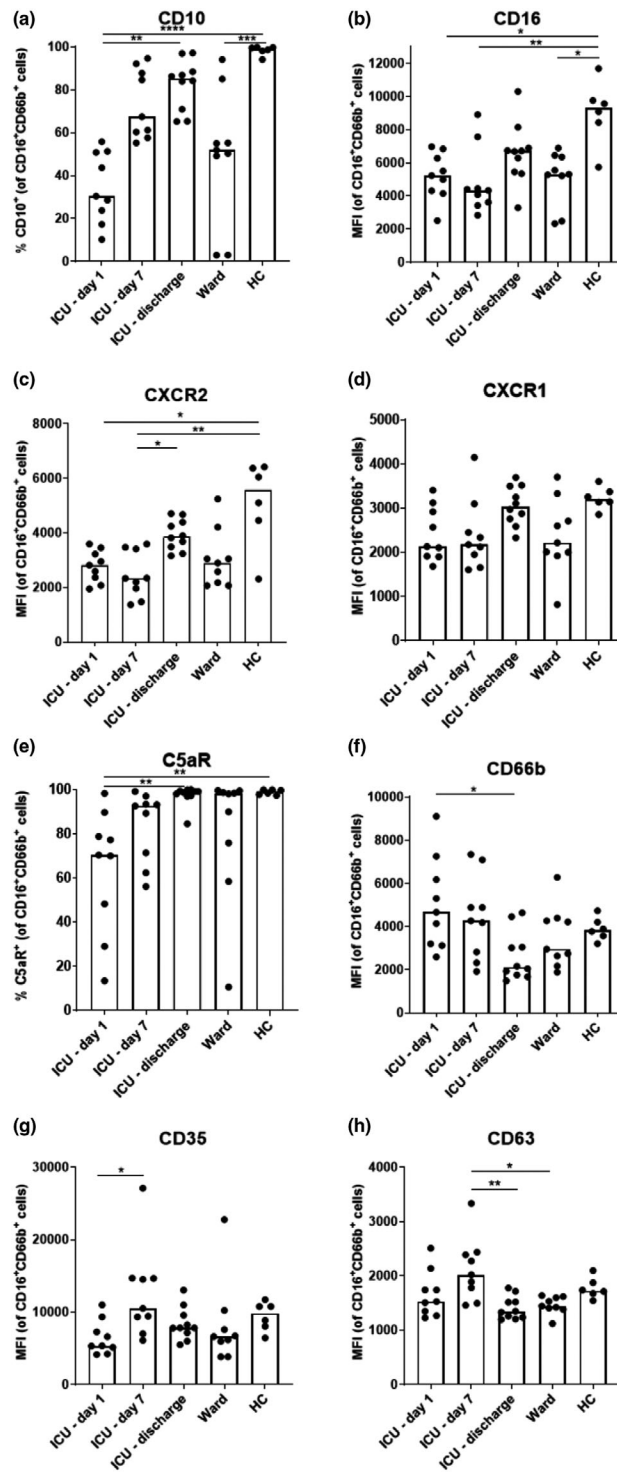
Figure 4. Phenotypical characterisation of peripheral blood neutrophils from patients with COVID-19. Flow cytometry was used to evaluate the surface expression of **(a)** CD10, **(b)** CD16, **(c)** CXCR2, **(d)** CXCR1, **(e)** C5aR, **(f)** CD66b, **(g)** CD35 and **(h)** CD63 on neutrophils (gated as CD16+CD66b+ cells) from COVID-19 patients who stayed at the ICU [samples were collected during the first 48 h after admission (ICU – day 1; $n = 9$), after one week (ICU – day 7; $n = 9$) and upon discharge from the ICU (ICU – discharge; $n = 10$)], COVID-19 patients who were hospitalised in general wards (ward; $n = 9$) and healthy controls (HC; $n = 6$). Results are represented as percentages of positive neutrophils or median fluorescence intensity (MFI). Bars indicate the median value for each study group. Results were statistically analysed by the Kruskal–Wallis with Dunn's multiple comparisons tests. *$P \leq 0.05$; **$P \leq 0.01$; ***$P \leq 0.001$; ****$P \leq 0.0001$.

validated in permissive Vero CCL81 cells (Figure 5a, b). Evaluation of the viral load in neutrophils 6 or 12 h post-infection revealed low static levels of viral RNA inside cells and in culture supernatant, and decreasing levels of infective SARS-CoV-2 in culture supernatant, indicating that SARS-CoV-2 is unable to replicate in human neutrophils *in vitro* (Figure 5c–e). In addition, microscopic evaluation of neutrophil cell cultures infected with SARS-CoV-2 confirmed the lack of virus-induced cytopathic effects or cell death (Figure 5f). Accordingly, the levels of lactate dehydrogenase (LDH) – that increase upon neutrophil death – in supernatant were not increased if cells were infected with SARS-CoV-2 as compared to vehicle-treated cells (Figure 5g). The assessment of MPO activity revealed similar enzymatic activities in supernatants from SARS-CoV-2-challenged and vehicle-treated neutrophils (Figure 5h). An increase in MPO release was observed from 6 to 12 h post-infection, but was similar between the virus- and vehicle-treated groups.

DISCUSSION

The COVID-19 pandemic has come on top of the annual death toll of infectious diseases and remains a significant risk to human health worldwide. The precise mechanisms underlying the heterogeneity of COVID-19 disease courses are incompletely understood, although an advanced age and/or the presence of comorbidities that provide a certain grade of chronic inflammation (e.g. diabetes, obesity) may promote rather unfavorable clinical outcomes. There is an urgent need to further elucidate the molecular and cellular mechanisms involved in progression from mild to life-threatening disease.

Lymphopenia is a near-uniform finding in severe cases of SARS-CoV-2 infection, like in several other viral infections, and typically coincides with profound alterations of the myeloid cell compartment, especially the depletion of $CD14^{low}CD16^{high}$ non-classical monocytes and the expansion of the proportion of circulating neutrophils.[30,31] High expression of T-cell-suppressing molecules programmed death ligand-1 and arginase-1 by neutrophils from COVID-19 patients may further contribute to T-cell malfunction.[30,32,33] The elevated NLR that we also observed in our patient population (Table 2) has appeared as an independent biomarker to predict poor clinical outcomes, supporting the notion that

neutrophils may play a pivotal role in COVID-19 pathogenesis.[15,34] Further experimental evidence favoring this hypothesis includes the presence of massive amounts of the neutrophil activation marker S100A8/A9 in the circulation of COVID-19 patients, which correlate positively with neutrophil numbers as well as disease severity and mortality.[31,35–37] Also, the aberrant formation of NETs may contribute to tissue damage and coagulopathy as seen in patients with severe COVID-19.[38,39]

These recent scientific findings sparked our interest to investigate in detail the kinetics of peripheral blood neutrophils from hospitalised COVID-19 patients. For this purpose, we had access to fresh blood samples (samples were processed typically within 30 min of withdrawal) and took advantage of an immunomagnetic purification method that allows for fast isolation of cells to minimise artefacts. The study population included patients who were hospitalised in dedicated general wards or in ICUs (Table 2). We compared the parameters with those from age- and sex-matched healthy individuals.

In line with a previously published report describing the presence of immature neutrophils in bronchoalveolar lavage fluid and in the circulation of COVID-19 patients,[31] we detected large numbers of immature neutrophils in the peripheral blood of ICU patients at the time of admission. The occurrence of these immature cells in the periphery indicates emergency myelopoiesis: a haematological response to severe systemic inflammation.[40,41] The observed high plasma levels of G-CSF may at least partially explain the presence of immature neutrophils in the periphery. Indeed, G-CSF is known to cause a 'shift to the left', that is the occurrence of immature neutrophils in peripheral blood, suggesting a pivotal role for this lineage-specific cytokine in emergency myelopoiesis.[16,42,43] Moreover, we detected increased levels of TIMP-1 in plasma from COVID-19 patients. In mice, increased TIMP-1 levels are known to stimulate enrichment of myeloid progenitors and upregulation of genes related to granulopoiesis.[44]

Neutrophil activation requires tight regulation to guarantee immune surveillance and to prevent deleterious immune activation leading to tissue damage.[45,46] Evaluation of the activation state of peripheral blood neutrophils from COVID-19

Table 2. COVID-19 patient characteristics

Characteristics	ICU patients (N = 67)	Ward patients (N = 48)
Age (years)	62 (54–69)	69 (58–81)
Sex		
Male	50/67 (74.6%)	26/48 (54.2%)
Female	17/67 (25.4%)	22/48 (45.8%)
BMI (kg/m^2)	28.2 (25.0–31.2)	26.4 (24.4–30.7)
Smoking history		
Active	5/67 (7.5%)	2/48 (4.2%)
Former	21/67 (31.3%)	17/48 (35.4%)
Never	24/67 (35.8%)	18/48 (37.5%)
Unknown	17/67 (25.4%)	11/48 (22.9%)
Co-morbidities		
Diabetes	16/67 (23.9%)	10/48 (20.8%)
Prior myocardial infarction	3/67 (4.5%)	3/48 (6.3%)
Congestive heart failure	1/67 (1.5%)	6/48 (12.5%)
History of arterial hypertension	34/67 (50.7%)	29/48 (60.4%)
Peripheral vascular disease	2/67 (3.0%)	1/48 (2.1%)
Chronic pulmonary disease	9/67 (13.4%)	7/48 (14.6%)
Rheumatologic disease	8/67 (11.9%)	5/48 (10.4%)
Renal disease	1/67 (1.5%)	3/48 (6.3%)
Malignancy	7/67 (10.4%)	8/48 (16.7%)
Symptoms at hospital admission		
Fever	40/67 (59.7%)	22/48 (45.8%)
Sore throat	3/67 (4.5%)	2/48 (4.2%)
Shortness of breath	44/67 (65.7%)	17/48 (35.4%)
Loss of smell and/or taste	6/67 (9.0%)	4/48 (8.3%)
Cough	36/67 (53.7%)	21/48 (43.8%)
Chest pain	8/67 (11.9%)	7/48 (14.6%)
Muscle pain (myalgia)	5/67 (7.5%)	4/48 (8.3%)
Fatigue/malaise	22/67 (32.8%)	21/48 (43.8%)
Headache	3/67 (4.5%)	3/48 (6.3%)
Vomiting/nausea	7/67 (10.4%)	6/48 (12.5%)
Diarrhoea	10/67 (14.9%)	10/48 (20.8%)
Time from onset of symptoms to hospital admission (days)	7 (5–9)	6 (3–9)
Length of ICU stay (days)	15 (8–29)	/
Length of total hospital stay (days)	28 (18–40)	8 (4–12)
Mortality	4/67 (6.0%)	2/48 (4.2%)

Characteristics	ICU – day 1 (N = 26)	ICU – day 7 (N = 42)	ICU – discharge (N = 50)	Ward (N = 48)
Respiratory support at time of sampling				
No oxygen needed	0/26 (0%)	0/42 (0%)	10/50 (20.0%)	17/48 (35.4%)
Oxygen	2/26 (7.6%)	3/42 (7.1%)	32/50 (64.0%)	30/48 (62.5%)
High flow oxygen support (Optiflow)	13/26 (50.0%)	8/42 (19.0%)	5/50 (10.0%)	0/48 (0%)
Mechanical ventilation	11/26 (42.3%)	24/42 (57.1%)	3/50 (6.0%)	1/48 (2.1%)
ECMO	0/26 (0%)	4/42 (9.5%)	0/50 (0%)	0/48 (0%)
Inhaled nitric oxide	0/26 (0%)	3/42 (7.1%)	0/50 (0%)	0/48 (0%)
Leukocyte count (*10^9 L^{-1})	8.5 (5.9–11.3)	8.9 (6.6–10.8)	9.1 (6.6–11.8)	6.1 (4.2–8.9)
Neutrophil count (*10^9 L^{-1})	6.4 (3.9–9.9)	7.0 (5.2–9.4)	6.5 (4.9–8.4)	4.6 (3.2–7.0)
Eosinophil count (*10^9 L^{-1})	0 (0–0)	0.1 (0–0.2)	0.2 (0.1–0.4)	0 (0–0.1)
Lymphocyte count (*10^9 L^{-1})	0.7 (0.4–1.0)	1.0 (0.6–1.4)	1.6 (1.2–2.4)	1.1 (0.8–1.3)
Neutrophil-to-lymphocyte ratio (NLR)	9.1	7	4.1	4.2
D-dimer (µg L^{-1})	859 (695–1408)	1718 (983–4534)	1456 (999–3861)	819 (515–1255)
CRP (mg L^{-1})	141.1 (73.6–257.1)	141.5 (38.5–253.1)	20.1 (11.6–34.6)	61.0 (28.1–114.9)
Treatment < 24 h of sampling				
Hydroxychloroquine	15/26 (57.7%)	2/42 (4.8%)	2/50 (4.0%)	34/48 (70.8%)

(Continued)

Table 2. Continued.

Characteristics	ICU − day 1 (*N* = 26)	ICU − day 7 (*N* = 42)	ICU − discharge (*N* = 50)	Ward (*N* = 48)
Azithromycin	0/26 (0%)	0/42 (0%)	0/50 (0%)	1/48 (2.1%)
Remdesivir	3/26 (11.5%)	0/42 (0%)	1/50 (2.0%)	0/48 (0%)
Tocilizumab	1/26 (3.8%)	1/42 (2.4%)	0/50 (0%)	0/48 (0%)
Anakinra	1/26 (3.8%)	1/42 (2.4%)	0/50 (0%)	0/48 (0%)
LMWH	25/26 (96.2%)	38/42 (90.5%)	49/50 (98.0%)	36/48 (75.0%)
Tranexamic acid	4/26 (15.4%)	12/42 (28.6%)	1/50 (2.0%)	0/48 (0%)
Corticosteroids	9/26 (34.6%)	20/42 (47.6%)	15/50 (30.0%)	4/48 (8.3%)

Continuous variables are expressed in median (interquartile range). Categorical variables are presented as counts (percentage).
General characteristics of all unique patients included in the study (67 ICU and 48 ward) are indicated in the first part of the table. Since it was not possible to collect all samples for every patient, the lower part of the table only contains the samples that were obtained at each time point (26 from ICU − day 1, 42 from ICU − day 7 and 50 from ICU − discharge).
BMI, body mass index; CRP, C-reactive protein; ECMO, extracorporeal membrane oxygenation; ICU, intensive care unit; LMWH, low-molecular-weight heparin.

patients revealed downregulation of CXCR2 and C5aR. Since chemoattractant receptors are internalised rapidly upon ligand-induced activation, the observed downregulation of these receptors potentially suggests neutrophil activation.[47,48] Additional evidence for the presence of highly activated neutrophils in the periphery of patients with severe COVID-19 is provided by the massive protein concentrations of neutrophil elastase, increased gelatinolytic activity in plasma and enhanced concentrations of circulating TIMP-1/MMP-9 complexes. Increased MMP-9 plasma levels were associated with mortality in COVID-19 patients.[37] Moreover, high plasma levels of the archetypal neutrophil-attracting chemokine CXCL8 and the myelopoietic cytokine G-CSF may contribute to the activation of peripheral neutrophils.[16,42,49] Strikingly, occasional high expression of CXCR3 − the receptor for the interferon-induced chemokines CXCL9, CXCL10 and CXCL11 − and CXCR4 was detected on neutrophils from ICU patients (Supplementary figure 2b). These receptors are not typically found on circulating neutrophils but can be upregulated in an inflamed environment (CXCR3) or appear on immature or aged neutrophils (CXCR4).[48] In addition, enhanced levels of CXCL10 and CXCL11, the two most potent CXCR3 ligands, and reduced activity of their deactivating enzyme CD26 were detected in plasma from COVID-19 patients. Noteworthy, former research efforts confirmed the expression of the *CXCR4* gene by neutrophils from COVID-19 patients.[31]

In interpreting the overall results of this study, we acknowledge that our sample size for analysis of patient neutrophils is small because of the practical limitations that come with neutrophil experiments, in particular the need of highly fresh blood samples. Moreover, patients were at different treatment strategies and had divergent comorbidities (Table 2). Artificial ventilation and other inherent aspects of admittance to ICU may induce changes in neutrophil function and responsiveness that we are unable to anticipate at this moment. Severe COVID-19 has a strong immunopathogenic component, and disease complexity prevents us from understanding to which stimulus the neutrophils are actually responding. In addition, the disease courses of individual patients were highly variable. Surprisingly, no significant differences in neutrophil phenotype or polarisation responses were found between patients with or without treatment with steroids. Moreover, in contrast to most other studies that use whole blood or rely on the accidental presence of neutrophils within the peripheral blood mononuclear cell (PBMC) layer, we analysed highly pure and freshly isolated neutrophils.[31,50]

Collectively, and for the first time, we report the kinetics of peripheral blood neutrophils and their products of activation. We demonstrate increased numbers of immature and activated neutrophils in the circulation from patients with severe COVID-19. These populations disappear towards discharge from ICU. Moreover, we show that SARS-CoV-2 is unable to replicate in human neutrophils *in vitro*, suggesting that neutrophils are unlikely to support SARS-CoV-2 replication in patients. The lack of evidence indicating infection or direct interaction between SARS-CoV-2 and neutrophils also suggests that phenotypical and functional changes observed in neutrophils from
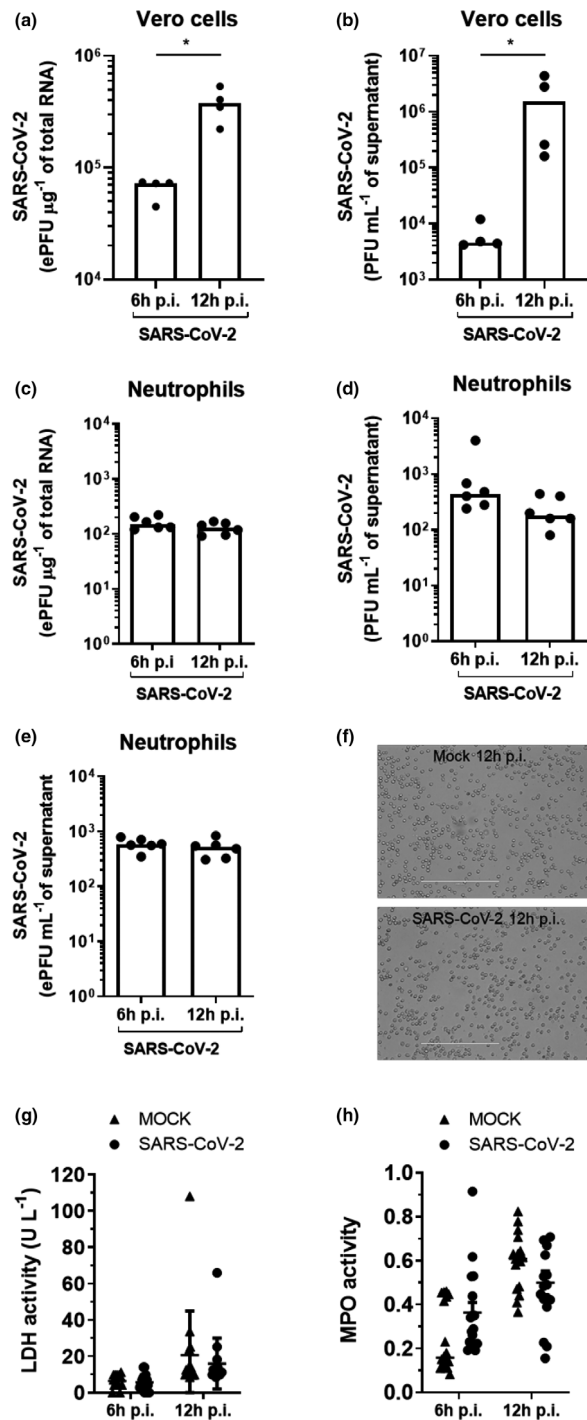
Figure 5. SARS-CoV-2 fails to replicate in human neutrophils and does not induce MPO release or cell death *in vitro*. **(c, d)** Neutrophils were isolated from the peripheral blood of healthy donors and immediately challenged with SARS-CoV-2 *in vitro* at a multiplicity of infection of 0.1 or vehicle-treated. **(a, b)** Vero cells were used as a positive control. At 6 and 12 h post-infection (p.i.), **(a, c)** cells and **(b, d, e)** supernatants were collected. Quantification of SARS-CoV-2 replication in **(a)** Vero cells, **(c)** neutrophils or **(e)** neutrophil cell culture supernatant by RT-qPCR and shown as equivalent of plaque-forming unit (ePFU) mL^{-1}. Plaque assays assessed infectious viral progeny in **(b)** Vero cells and **(d)** neutrophil supernatant in PFU mL^{-1}. **(f)** Bright-field microscopy images at 12 h p.i. of SARS-CoV-2-infected and mock-infected neutrophil cultures. **(g)** LDH activity and **(h)** MPO activity were assessed 6 and 12 h p.i. in neutrophil culture supernatants. Each dot represents an independent measurement. Bars indicate median values. Samples were statistically analysed using the Mann–Whitney *U*-test or analysis of variance (ANOVA) with Sidak's multiple comparison's tests.

Table 3. Overview of antibodies used for flow cytometry

Human antigen	Clone	Label	Host species	Company
CD10	HI10a	BV786	Mouse	BD Biosciences
CD11b	ICRF44	BV510	Mouse	BD Biosciences
CD11b	ICRF44	APC-Cy7	Mouse	BioLegend
CD11c	3.9	eFluor 710	Mouse	eBioscience
CD15	HI98	BUV395	Mouse	BD Biosciences
CD15	W6D3	BV786	Mouse	BD Biosciences
CD16	3G8	Alexa Fluor 700	Mouse	BD Biosciences
CD16	3G8	BUV395	Mouse	BD Biosciences
CD35	E11	FITC	Mouse	BioLegend
CD49d	9F10	BV711	Mouse	BioLegend
CD54	HA58	BV711	Mouse	BD Biosciences
CD62L	DREG56	APC	Mouse	eBioscience
CD63	H5C6	BV510	Mouse	BD Biosciences
CD66b	G10F5	BV421	Mouse	BD Biosciences
CD66b	G10F5	PerCP-Cy5.5	Mouse	BioLegend
CD88 (C5aR)	S5/1	PerCP-Cy5.5	Mouse	BioLegend
CD181 (CXCR1)	5A12	PE	Mouse	BD Biosciences
CD182 (CXCR2)	6C6	FITC	Mouse	BD Biosciences
CD183 (CXCR3)	1C/CXCR3	BUV395	Mouse	BD Biosciences
CD184 (CXCR4)	12G5	BUV395	Mouse	BD Biosciences
CD191 (CCR1)	53 504	Alexa Fluor 647	Mouse	BD Biosciences
CD192 (CCR2)	K036C2	Alexa Fluor 488	Mouse	BioLegend
IL-1R1	FAB269P	PE	Mouse	R&D Systems
IL-1R2	REA744	FITC	Mouse	Miltenyi Biotec
BLTR1	203/14F11	BV510	Mouse	BD Biosciences
FPR1	5F1	Alexa Fluor 647	Mouse	BD Biosciences
HLA-DR	L243	BV650	Mouse	BioLegend

APC, allophycocyanin; BLTR1, leukotriene B4 receptor 1; BUV, Brilliant UltraViolet; BV, Brilliant Violet; FITC, fluorescein isothiocyanate; FPR, formyl peptide receptor; HLA, human leucocyte antigen; PE, phycoerythrin; PerCP, peridinin–chlorophyll protein complex.

COVID-19 patients are indirect consequences of SARS-CoV-2 infection *in vivo*. We speculate that the high concentrations of circulating pro-inflammatory cytokines and chemokines are at least partially responsible for the altered activation/maturation states of neutrophils in the blood of patients with severe COVID-19. In turn, activated neutrophils contribute to persistent and potentially harmful immune responses if patients are not treated appropriately.

METHODS

Patients

Patients were recruited at the University Hospital Leuven. Blood samples were collected from ICU patients during the first 48 h after admission, after one week (between days 6 and 8) and upon discharge from the ICU. In addition, samples were collected from patients upon admission to general wards. Blood samples from age- and sex-matched healthy individuals were investigated for comparative purposes. For analysis of neutrophils and plasma, blood samples were collected in vacutainer tubes treated with ethylenediaminetetraacetic acid (EDTA) or with sodium citrate, respectively (BD Biosciences, Franklin Lakes, NJ) (refer to Table 2 for detailed characteristics of patients). Due to the limited availability of plasma and fresh blood within 30 min of withdrawal, not all patient samples could be included at each time point and in every experiment performed.

Plasma collection

Blood samples were spun down for 10 min at 400 g. The supernatant was collected and centrifuged for 20 min at 16 000 g to obtain platelet-free plasma. Plasma was stored until further use at $-80°C$.

Isolation of neutrophils

Neutrophils used in shape change assays and for phenotypical characterisation were isolated from the whole blood by immunomagnetic negative selection (EasySep™ Direct Human Neutrophil Isolation Kit; Stemcell Technologies, Vancouver, Canada) within 30 min of withdrawal. Information on neutrophil purity is included in Supplementary figure 3a. Neutrophils used in SARS-CoV-2 exposure assays were isolated from fresh peripheral blood

of healthy donors by centrifugation in a density gradient (Ficoll-Paque™ PLUS; Cytiva, MA, USA). Erythrocytes were removed with ammonium–chloride–potassium (ACK) lysing buffer (Thermo Fisher Scientific, Waltham, MA, USA).

Phenotypical analysis

Neutrophils were treated with FcR block (Miltenyi Biotec, Bergisch Gladbach, Germany) and Fixable Viability Stain 620 (BD Biosciences) or Zombie Aqua 516 (BioLegend, San Diego, CA, USA) for 15 min at room temperature. Subsequently, cells were washed with flow cytometry buffer [PBS + 2% (*v/v*) foetal calf serum (FCS) + 2 mM EDTA] and stained with fluorescently labelled antibodies. Antibodies used in this study were titrated in-house and are listed in Table 3. Following incubation for 25 min (on ice), cells were washed with flow cytometry buffer and fixed with BD Cytofix (BD Biosciences). Results were analysed using a BD LSRFortessa™ X-20 (BD Biosciences) equipped with DIVA software (BD Biosciences). FlowJo software (BD Biosciences) was used for downstream analysis. Neutrophils were gated as $CD16^+CD66b^+$ cells within the population of living single cells (Supplementary figure 3b).

Shape change assay

Neutrophils were suspended in shape change buffer (1X HBSS without Ca^{2+} and Mg^{2+} and supplemented with 10 mM HEPES) at a concentration of 0.6×10^6 cells mL^{-1}. The cell suspension (50 μL) was added to 50 μL of chemoattractant dilution and incubated for 0 or 3 min in a flat-bottom 96-well plate followed by fixation with 100 μL Cytofix (BD Biosciences). The following chemoattractants were used: recombinant CXCL8 (72AA; PeproTech, Rocky Hill, NJ, USA; final concentration of 5 or 12.5 ng mL^{-1}), recombinant CXCL10 (PeproTech; final concentration of 100 or 300 ng mL^{-1}), chemically synthesised CXCL12α (final concentration of 300 ng mL^{-1})[51] and TNF-α (PeproTech; final concentration of 50 ng mL^{-1}). Cells were analysed by microscopic evaluation of the cellular shape. Two independent researchers performed the assessment.

Quantification of cytokines, chemokines, enzymes and enzyme inhibitors

Plasma concentrations of G-CSF, GM-CSF, CXCL1, CXCL5, CXCL8, CXCL11 and CXCL12α were measured using customised Meso Scale Discovery (Rockville, MD, USA) multiplex assays. CXCL10 concentrations were evaluated using a specific sandwich ELISA developed in our laboratory. Neutrophil elastase, TIMP-1, TIMP-1/MMP-9 complexes and α2M were quantified by commercially available DuoSet ELISAs (R&D Systems, Minneapolis, MN, USA).

Measurement of gelatinolytic and MMP activity

To test metalloproteinase and gelatinase activity, 15 μL of a mixture of dye-quenched (DQ) gelatin (DQ™ Gelatin;

Invitrogen, Carlsbad, CA, USA) (final concentration of 3 μg mL^{-1}) and OMNIMMP substrate peptide (Mca-PLGL-Dpa-AR-NH$_2$, Cat. No. BML-P126-0001; Enzo Life Sciences, Farmingdale, NY, USA) (final concentration of 6 μg mL^{-1}) in assay buffer [50 mM Tris, 150 mM NaCl, 5 mM $CaCl_2$, 0.01% Tween-20, pH 7.4] was added to 5 μL plasma. Fluorescence was measured over time with the CLARIOstar microplate reader (BMG LABTECH, Ortenberg, Germany). Metalloproteinase activity was inhibited by the addition of 100 mM EDTA. All data shown are representative for the fluorescence measured after 1 h incubation at 37°C.

Measurement of CD26 activity

CD26 activity was quantified using a colorimetric assay. Plasma samples were diluted 1:20 in 75 mM Tris-HCl (pH 8.3) containing 500 μM of the chromogenic substrate Gly-Pro p-nitroanilide p-toluenesulfonate (GP-p-NA; Sigma-Aldrich, Saint Louis, MO, USA) in a flat-bottom 96-well plate (final volume of 200 μL per well). The enzymatic conversion of GP-p-NA to p-NA was measured every 15 min for 12 h at 37°C. CD26 enzymatic activity (U L^{-1}) was calculated based on the absorbance values at 405 nm and the Lambert–Beer law [extinction coefficient of p-NA = 9500 M^{-1} cm^{-1}; path length = 0.625 cm (200 μL) in a 96-well plate].

Virus and production of viral stocks

The SARS-CoV-2 strain HIAE-02 SARS-CoV-2/SP02/human/2020/BRA (GenBank Accession Number MT126808.1), isolated from the second patient diagnosed with COVID-19 in Brazil, was kindly provided by Prof. Edison Luiz Durigon (University of São Paulo, Brazil). SARS-CoV-2 stocks were produced by Vero CCL81 cells. The viral stock titre and identity were assessed by a viral plaque assay and RT-qPCR.

In vitro infection of cells with SARS-CoV-2

All experiments involving manipulation of infective SARS-CoV-2 were performed in the BSL3 facility of the Laboratory of Emerging Viruses (University of Campinas, Brazil). Purified neutrophils or Vero CCL81 cells were seeded in 24-well plates (1×10^6 cells per well) and incubated with SARS-CoV-2 at a multiplicity of infection of 0.1 for 1 h at 37°C and 5% CO_2. Plates were centrifuged, the viral inoculate was removed and replaced by RPMI medium supplemented with 10% (*v/v*) FCS and 1% (*w/v*) penicillin–streptomycin. Samples were collected 6 or 12 h post-infection.

Measurement of peroxidase and LDH activity

The collected cell supernatants (*vide supra*) were exposed to UV radiation for 15 min to neutralise viral activity. A mixture containing equal amounts of Color Reagent A and Color Reagent B (R&D Systems) was added to each well of a 96-well plate together with 50 μL of supernatant sample to assess peroxidase activity. Data were acquired at 450 nm in an EnSpire Plate Reader (PerkinElmer, Waltham, MA, USA).

The assessment of extracellular LDH activity was performed using the LDH Liquiform Kit (Labtest, Lagoa Santa, Brazil) according to the manufacturer's protocol and read at 340 nm using the EnSpire Plate Reader.

Viral RNA extraction and quantification by RT-qPCR

RNA was extracted from cell extracts using the Quick-RNA Viral Kit (Zymo Research, Irvine, CA), according to the manufacturer's recommendations. RNA quality and quantity were verified with a NanoDrop One Spectrophotometer (Thermo Fisher Scientific). SARS-CoV-2 RNA quantification was performed by RT-qPCR according to the Charité protocol[52] using primers and probes for the E gene (forward: 5′-ACA GGT ACG TTA ATA GTT AAT AGC GT-3′, reverse: 5′-ATA TTG CAG CAG TAC GCA TAC GCA CAC A-3′, probe: 5′-6FAM-ACA CTA GCC ATC CTT ACT GCG CTT CG-QSY-3′). All reactions were assembled in a final volume of 12 μL containing 3 μL of TaqMan Fast Virus 1-Step Master Mix (Applied Biosystems, Foster City, CA, USA), 800 nᴍ primers, 400 nᴍ probe and 6 μL of 100-fold diluted RNA in ultrapure water. The cycling algorithm used in this study was as follows: 1 cycle at 50°C for 10 min, 1 cycle at 95°C for 2 min, followed by 45 cycles at 95°C for 5 s and 60°C for 30 s in the QuantStudio3 System (Applied Biosystems). All applicable measures were taken to prevent cross-contamination of samples, and negative and positive controls were included. Reference values for equivalents of plaque-forming unit (ePFU) calculation are Ct means of samples with known viral load (in PFU mL^{-1}) plotted as a standard curve.

ACKNOWLEDGMENTS

CONFLICT OF INTEREST

The authors declare that no conflict of interest exists.

AUTHOR CONTRIBUTION

Mieke Metzemaekers: Conceptualization; Data curation; Formal analysis; Funding acquisition; Investigation; Methodology; Validation; Visualization; Writing-original draft; Writing-review & editing. **Seppe Cambier:** Conceptualization; Data curation; Formal analysis; Investigation; Methodology; Writing-original draft; Writing-review & editing. **Marfa Blanter:** Data curation; Formal analysis; Investigation; Methodology; Writing-review & editing. **Jennifer Vandooren:** Data curation; Formal analysis; Investigation; Methodology; Writing-review & editing. **Ana Carolina de Carvalho:** Formal analysis; Investigation; Methodology; Writing-review & editing. **Bert Malengier-Devlies:** Formal analysis; Investigation; Methodology; Writing-review & editing. **Lore Vanderbeke:** Conceptualization; Data curation; Investigation; Writing-review & editing. **Cato Jacobs:** Data curation; Investigation; Writing-review & editing. **Sofie Coenen:** Data curation; Investigation; Writing-review & editing. **Erik Martens:** Formal analysis; Methodology; Writing-review & editing. **Noëmie Pörtner:** Formal analysis; Investigation; Writing-review & editing. **Lotte Vanbrabant:** Formal analysis; Investigation; Writing-review & editing. **Pierre Van Mol:** Data curation; Investigation; Writing-review & editing. **Yannick Van Herck:** Conceptualization; Data curation; Writing-review & editing. **Nathalie Van Aerde:** Data curation; Writing-review & editing. **Greet Hermans:** Data curation; Supervision; Writing-review & editing. **Jan Gunst:** Data curation; Investigation; Resources; Supervision; Writing-review & editing. **Alexandre Borin:** Formal analysis; Writing-review & editing. **Bruna Toledo N. Pereira:** Formal analysis; Writing-review & editing. **Arilson Bernardo dos SP Gomes:** Formal analysis; Writing-review & editing. **Stéfanie Primon Muraro:** Formal analysis; Writing-review & editing. **Gabriela Fabiano de Souza:** Formal analysis; Writing-review & editing. **Alessandro S Farias:** Data curation; Formal analysis; Writing-review & editing. **José Luiz Proenca-Modena:** Formal analysis; Writing-review & editing. **Marco Vinolo:** Formal analysis; Writing-review & editing. **Contagious Consortium:** Data curation; Writing-review & editing. **Pedro Elias Marques:** Conceptualization; Data curation; Writing-review & editing. **Carine Wouters:** Conceptualization; Data curation; Funding acquisition; Supervision; Writing-review & editing. **Els Wauters:** Conceptualization; Data curation; Funding acquisition; Investigation; Supervision; Writing-review & editing. **Sofie Struyf:** Data curation; Formal analysis; Funding acquisition; Investigation; Supervision; Writing-review & editing. **Patrick Matthys:** Conceptualization; Data curation; Formal analysis; Funding acquisition; Supervision; Writing-review & editing. **Ghislain Opdenakker:** Conceptualization; Data curation; Formal analysis; Supervision; Writing-review & editing. **Rafael Elias Marques:** Conceptualization; Data curation; Formal analysis; Funding acquisition; Investigation; Methodology; Writing-review & editing. **Joost Wauters:** Conceptualization; Data curation; Funding acquisition; Supervision; Writing-review & editing. **Mieke Gouwy:** Conceptualization; Data curation; Formal analysis; Investigation; Methodology; Supervision; Writing-review & editing. **Paul Proost:** Conceptualization; Data curation; Funding acquisition; Investigation; Methodology; Project administration; Resources; Supervision; Validation; Writing-review & editing.

ETHICAL APPROVAL

Written informed consent was obtained from all participants or their legal representatives according to the ethical guidelines of the Declaration of Helsinki. The Ethics

Committee of the University Hospital Leuven approved this study (S63881).

REFERENCES

1. Hoffmann M, Kleine-Weber H, Schroeder S *et al*. SARS-CoV-2 cell entry depends on ACE2 and TMPRSS2 and is blocked by a clinically proven protease inhibitor. *Cell* 2020; **181**: 271–280.e8.
2. Guan W-J, Ni Z-Y, Hu Y *et al*. Clinical characteristics of coronavirus disease 2019 in China. *N Engl J Med* 2020; **382**: 1708–1720.
3. Wu Z, McGoogan JM. Characteristics of and important lessons from the Coronavirus Disease 2019 (COVID-19) outbreak in China: summary of a report of 72 314 cases from the Chinese center for disease control and prevention. *JAMA* 2020; **323**: 1239–1242.
4. Qin C, Zhou L, Hu Z *et al*. Dysregulation of immune response in patients with coronavirus 2019 (COVID-19) in Wuhan, China. *Clin Infect Dis* 2020; **71**: 762–768.
5. Huang C, Wang Y, Li X *et al*. Clinical features of patients infected with 2019 novel coronavirus in Wuhan, China. *Lancet* 2020; **395**: 497–506.
6. Wichmann D, Sperhake J-P, Lütgehetmann M *et al*. Autopsy findings and venous thromboembolism in patients with COVID-19: a prospective cohort study. *Ann Intern Med* 2020; **173**: 268–277.
7. Terpos E, Ntanasis-Stathopoulos I, Elalamy I *et al*. Hematological findings and complications of COVID-19. *Am J Hematol* 2020; **95**: 834–847.
8. Zhou F, Yu T, Du R *et al*. Clinical course and risk factors for mortality of adult patients with COVID-19 in Wuhan, China: a retrospective cohort study. *Lancet* 2020; **395**: 1054–1062.
9. Henry BM, de Oliveira MHS, Benoit S, Plebani M, Lippi G. Hematologic, biochemical and immune biomarker abnormalities associated with severe illness and mortality in coronavirus disease 2019 (COVID-19): a meta-analysis. *Clin Chem Lab Med* 2020; **58**: 1021–1028.
10. Li S, Jiang L, Li X *et al*. Clinical and pathological investigation of patients with severe COVID-19. *JCI insight* 2020; **5**: e138070.
11. Moore JB, June CH. Cytokine release syndrome in severe COVID-19. *Science* 2020; **368**: 473–474.
12. Zhang J-J, Dong X, Cao Y-Y *et al*. Clinical characteristics of 140 patients infected with SARS-CoV-2 in Wuhan, China. *Allergy* 2020; **75**: 1730–1741.
13. Liu J, Liu Y, Xiang P *et al*. Neutrophil-to-lymphocyte ratio predicts critical illness patients with 2019 coronavirus disease in the early stage. *J Transl Med* 2020; **18**: 206.
14. Ciccullo A, Borghetti A, Zileri Dal Verme L *et al*. Neutrophil-to-lymphocyte ratio and clinical outcome in COVID-19: a report from the Italian front line. *Int J Antimicrob Agents* 2020; **56**: 106017.
15. Gan J, Li J, Li S, Yang C. Leucocyte subsets effectively predict the clinical outcome of patients with COVID-19 pneumonia: a retrospective case-control study. *Front public Heal* 2020; **8**: 299.
16. Opdenakker G, Fibbe WE, Van Damme J. The molecular basis of leukocytosis. *Immunol Today* 1998; **19**: 182–189.
17. Adrover JM, Del Fresno C, Crainiciuc G *et al*. A neutrophil timer coordinates immune defense and vascular protection. *Immunity* 2019; **50**: 390-402.e10.
18. Mantovani A, Cassatella MA, Costantini C, Jaillon S. Neutrophils in the activation and regulation of innate and adaptive immunity. *Nat Rev Immunol* 2011; **11**: 519–531.
19. Cassatella MA, Östberg NK, Tamassia N, Soehnlein O. Biological roles of neutrophil-derived granule proteins and cytokines. *Trends Immunol* 2019; **40**: 648–664.
20. Deniset JF, Kubes P. Neutrophil heterogeneity: *Bona fide* subsets or polarization states? *J Leukoc Biol* 2018; **103**: 829–838.
21. Silvestre-Roig C, Fridlender ZG, Glogauer M, Scapini P. Neutrophil diversity in health and disease. *Trends Immunol* 2019; **40**: 565–583.
22. Hidalgo A, Chilvers ER, Summers C, Koenderman L. The neutrophil life cycle. *Trends Immunol* 2019; **40**: 584–597.
23. Suratt BT, Petty JM, Young SK *et al*. Role of the CXCR4/SDF-1 chemokine axis in circulating neutrophil homeostasis. *Blood* 2004; **104**: 565–571.
24. Lambeir AM, Proost P, Durinx C *et al*. Kinetic investigation of chemokine truncation by CD26/dipeptidyl peptidase IV reveals a striking selectivity within the chemokine family. *J Biol Chem* 2001; **276**: 29839–29845.
25. Vanderbeke L, Van Mol P, Van Herck Y *et al*. Monocyte-driven atypical cytokine storm and aberrant neutrophil activation as key mediators of COVID-19 disease severity. 2020. https://doi.org/10.21203/rs.3.rs-60579/v1.
26. Marini O, Costa S, Bevilacqua D *et al*. Mature CD10$^+$ and immature CD10$^-$ neutrophils present in G-CSF-treated donors display opposite effects on T cells. *Blood* 2017; **129**: 1343–1356.
27. Arebro J, Ekstedt S, Hjalmarsson E, Winqvist O, Kumlien Georén S, Cardell L-O. A possible role for neutrophils in allergic rhinitis revealed after cellular subclassification. *Sci Rep* 2017; **7**: 43568.
28. Manz MG, Boettcher S. Emergency granulopoiesis. *Nat Rev Immunol* 2014; **14**: 302–314.
29. Jung K-K, Liu X-W, Chirco R, Fridman R, Kim H-RC. Identification of CD63 as a tissue inhibitor of metalloproteinase-1 interacting cell surface protein. *EMBO J* 2006; **25**: 3934–3942.
30. Schulte-Schrepping J, Reusch N, Paclik D *et al*. Severe COVID-19 is marked by a dysregulated myeloid cell compartment. *Cell* 2020; **182**: 1419–1440.
31. Silvin A, Chapuis N, Dunsmore G *et al*. Elevated calprotectin and abnormal myeloid cell subsets discriminate severe from mild COVID-19. *Cell* 2020; **182**: 1401–1418.
32. Bronte V, Serafini P, Mazzoni A, Segal DM, Zanovello P. L-arginine metabolism in myeloid cells controls T-lymphocyte functions. *Trends Immunol* 2003; **24**: 302–306.
33. Bowers NL, Helton ES, Huijbregts RPH, Goepfert PA, Heath SL, Hel Z. Immune suppression by neutrophils in HIV-1 infection: role of PD-L1/PD-1 pathway. *PLoS Pathog* 2014; **10**: e1003993.
34. Yang A-P, Liu J-P, Tao W-Q, Li H-M. The diagnostic and predictive role of NLR, d-NLR and PLR in COVID-19 patients. *Int Immunopharmacol* 2020; **84**: 106504.

35. Wang S, Song R, Wang Z, Jing Z, Wang S, Ma J. S100A8/A9 in inflammation. *Front Immunol* 2018; **9**: 1298.

36. Shi H, Zuo Y, Yalavarthi S *et al*. Neutrophil calprotectin identifies severe pulmonary disease in COVID-19. *J Leukoc Biol* 2021; **109**: 67–72.

37. Abers MS, Delmonte OM, Ricotta EE *et al*. An immune-based biomarker signature is associated with mortality in COVID-19 patients. *JCI Insight* 2020; **6**: 144455.

38. Barnes BJ, Adrover JM, Baxter-Stoltzfus A *et al*. Targeting potential drivers of COVID-19: Neutrophil extracellular traps. *J Exp Med* 2020; **217**: e20200652.

39. Schönrich G, Raftery MJ, Samstag Y. Devilishly radical NETwork in COVID-19: Oxidative stress, neutrophil extracellular traps (NETs), and T cell suppression. *Adv Biol Regul* 2020; **77**: 100741.

40. Boettcher S, Manz MG. Sensing and translation of pathogen signals into demand-adapted myelopoiesis. *Curr Opin Hematol* 2016; **23**: 5–10.

41. Schultze JL, Mass E, Schlitzer A. Emerging principles in myelopoiesis at homeostasis and during infection and inflammation. *Immunity* 2019; **50**: 288–301.

42. van Os R, van Schie MLJ, Willemze R, Fibbe WE. Proteolytic enzyme levels are increased during granulocyte colony-stimulating factor-induced hematopoietic stem cell mobilization in human donors but do not predict the number of mobilized stem cells. *J Hematother Stem Cell Res* 2002; **11**: 513–521.

43. Kaushansky K. Lineage-specific hematopoietic growth factors. *N Engl J Med* 2006; **354**: 2034–2045.

44. Kobuch J, Cui H, Grünwald B, Saftig P, Knolle PA, Krüger A. TIMP-1 signaling via CD63 triggers granulopoiesis and neutrophilia in mice. *Haematologica* 2015; **100**: 1005–1013.

45. Ley K, Hoffman HM, Kubes P *et al*. Neutrophils: New insights and open questions. *Sci Immunol* 2018; **3**: eaat4579.

46. Liew PX, Kubes P. The neutrophil's role during health and disease. *Physiol Rev* 2019; **99**: 1223–1248.

47. Borroni EM, Mantovani A, Locati M, Bonecchi R. Chemokine receptors intracellular trafficking. *Pharmacol Ther* 2010; **127**: 1–8.

48. Metzemaekers M, Gouwy M, Proost P. Neutrophil chemoattractant receptors in health and disease: double-edged swords. *Cell Mol Immunol* 2020; **17**: 433–450.

49. Russo RC, Garcia CC, Teixeira MM, Amaral FA. The CXCL8/IL-8 chemokine family and its receptors in inflammatory diseases. *Expert Rev Clin Immunol* 2014; **10**: 593–619.

50. Wilk AJ, Rustagi A, Zhao NQ *et al*. A single-cell atlas of the peripheral immune response in patients with severe COVID-19. *Nat Med* 2020; **26**: 1070–1076.

51. Janssens R, Mortier A, Boff D *et al*. Natural nitration of CXCL12 reduces its signaling capacity and chemotactic activity *in vitro* and abrogates intra-articular lymphocyte recruitment *in vivo*. *Oncotarget* 2016; **7**: 62439–62459.

52. Corman VM, Landt O, Kaiser M *et al*. Detection of 2019 novel coronavirus (2019-nCoV) by real-time RT-PCR. *Eurosurveillance* 2019; **25**: 2000045.

Appendix 1
Additional Contagious consortium members

Alexander Wilmer (Laboratory for Clinical Infectious and Inflammatory Disorders, Department of Microbiology, Immunology and Transplantation, KU Leuven, Leuven, Belgium), Philippe Meersseman (Laboratory for Clinical Infectious and Inflammatory Disorders, Department of Microbiology, Immunology and Transplantation, KU Leuven, Leuven, Belgium), Diether Lambrechts (Laboratory of Translational Genetics, Department of Human Genetics, VIB-KU Leuven, Leuven, Belgium), Michael Casaer (Laboratory of Intensive Care Medicine, Department of Cellular and Molecular Medicine, KU Leuven, Leuven, Belgium), Steffen Rex (Anesthesiology and Algology, Department of Cardiovascular Sciences, KU Leuven, Leuven, Belgium), Nathalie Lorent (Department of Pneumology, University Hospitals Leuven, Leuven, Belgium), Karin Thevissen (Centre of Microbial and Plant Genetics, Department of Microbial and Molecular Systems (M2S), KU Leuven, Leuven, Belgium), Kim Martinod (Centre for Molecular and Vascular Biology, Department of Cardiovascular Sciences, KU Leuven, Leuven, Belgium).

Supporting Information

Additional supporting information may be found online in the Supporting Information section at the end of the article.